

# Wavefunction Masking and Strong-Field Double Ionization

S. L. Haan

*Department of Physics and Astronomy, Calvin College, Grand Rapids, MI 49546, USA*

e-mail: haan@calvin.edu

Received February 7, 2005

**Abstract**—We present details of the quantum-mechanical technique of masking and show its usefulness for tracking various quantum trajectories toward double ionization (DI) in intense laser fields. We consider slowdown and speedup recollision processes, and we show that quantum interference among various trajectories has minimal effect. We show how sequential masking can be employed to show that the DI visible in our plots originates from recollision. In addition, we show how masks that break the electron-exchange symmetry can be useful for providing classical descriptions that distinguish between the inner and the outer electron in recollision. The symmetry-violating wavefunctions show that electron interchange can occur, with the returning electron being recaptured and the other electron escaping. They also show that, in typical slowdown collisions that lead to double ionization, the returning electron recollides with the inner electron, overshoots the nucleus, and is then pushed back by the laser field so that it follows the other electron away from the core in the direction of the laser force. This sequence agrees with classical ensemble results.

## 1. INTRODUCTION

It is a privilege for me to be able to contribute to this special issue that honors Professor J.H. Eberly. He and I began collaborating in 1992–1993 when I spent a sabbatical at the University of Rochester working with him and his postdoctoral assistant Rainer Grobe, who is now a professor at Illinois State University. Our work focused on the “aligned-electron” model of helium [1], in which the motions of the electrons are constrained to be parallel with the polarization of the laser field. Professor Eberly’s group had experienced great success with the analogous one-electron model [2] that they had introduced to study processes in strong laser fields, as I believe is discussed elsewhere in this special issue in articles by Javaneinen, Grobe, and Su [3]. Shortly before my arrival, Eberly and Grobe had been gaining insights into electron–electron correlation from the aligned-electron model for  $H^-$  [4], and we were eager to learn the structure of model helium and to begin to use it to study two-electron processes in strong fields. It is now more than twelve years later, Professor Eberly and I are still collaborating, and the model—sometimes referred to as “ $Z = 2$  Eberlonium”—is still providing rich insights into two-electron processes in strong laser fields for numerous groups around the world [5]. Through the years various persons have worked with Professor Eberly and myself on the project, including Rochester postdoctoral researchers Wei-Chih Liu and Carsten Szymanowski and graduate students Raphael Panfili and Phay Ho. The collaboration has also involved numerous undergraduate students at Calvin College.

I cannot overstate how valuable our collaboration has been to me. It has kept me from becoming isolated or bogged down. Professor Eberly has been a wonderful collaborator, someone I could bounce ideas off and

who gives me honest appraisals of work accomplished and of what is important. The expertise of his postdoctoral assistants and graduate students has been valuable not only for idea sharing but also for keeping programming glitches from becoming serious obstacles. I write this paper with considerable gratitude for their willingness to collaborate with me. The value of the collaboration extends beyond the professional; I consider Joe a good friend and I have genuinely enjoyed working with him.

The present paper relates to the dynamics of strong-field nonsequential double ionization (DI) of atoms, as revealed by the aligned-electron model. The work employs and discusses the quantum-mechanical technique that Professor Eberly has dubbed “masking.” The technique, which Professor Eberly and I introduced in a joint presentation at Laser Physics 2000 in Bordeaux, France, and which we discuss in [6], exploits the simplicity and flexibility of the aligned-electron model. As indicated by Professor Eberly in that Bordeaux talk, truncating the physics so as to include only the essential motion in the direction of the laser field allows for rapid testing of ideas and comparison of theory with experiment, sometimes allowing us to quickly discard erroneous ideas after performing a few simple tests. Also, working with a simple, flexible model can help us to develop an intuitive “feel” for the dynamics, so that we can know what to look for as we move to more complex models. Of course, there is always the possibility that a conclusion reached in a simple model will not be borne out in a more complicated model, but even then we can learn something. Thus, the use of the model has nicely complemented the studies of DI through other theoretical means, such as S-matrix formalism [7] and full three-dimensional calculations [8].

Several students have been involved in the component of the project presented here, most notably

Dr. Raphael Panfili of Rochester and my undergraduate researcher Klaas Hoekema. They, along with Professor Eberly, are due special acknowledgment as contributors to the techniques and ideas in this paper.

## 2. THE MODEL

The aligned-electron model allows electron motion only parallel or antiparallel to the laser field. In atomic units, the full Hamiltonian for the system is

$$H(x_1, x_2) = p_1^2/2 + p_2^2/2 - 2/(x_1^2 + 1)^{1/2} - 2/(x_2^2 + 1)^{1/2} + 1/[(x_1 - x_2)^2 + 1]^{1/2} + (x_1 + x_2)E_0 f(t) \sin(\omega t),$$

where  $x_1$  and  $x_2$  denote positions of the two electrons,  $p_1$  and  $p_2$  denote the momenta,  $E_0$  is the maximum electric field strength,  $\omega$  is the laser (angular) frequency, and  $f(t)$  is a pulse-shape function, which we take to be trapezoidal with a two-cycle turn-on and two-cycle turn-off. We start the system in its ground state and develop it on a numerical grid that typically extends to  $\pm 400$  au for each electron. We use absorbing boundaries near the edges of the box to prevent wraparound. Throughout this paper we use the laser intensity  $6.5 \times 10^{14}$  W/cm<sup>2</sup> and frequency  $\omega = 0.0584$  au.

Our choice of laser parameters places the ionization in the knee area of DI (see [9] for a review), where experimental studies [10] have revealed that orders of magnitude more DI occurs than would be expected for independently behaving electrons [11]. This excess DI is understood to arise primarily from recollision. The standard simple man's description of recollision [12] is a mixture of quantum and classical physics, with one electron tunneling from the atomic core and then oscillating within the external laser field in a very classical fashion. If it returns to the core, it can recollide with the inner electron and ionize it. It would be very desirable to do a fully quantum-mechanical solution of the time-dependent Schrödinger equation for the system, but doing so is a monumental task [8]. Fortunately, it is not such a monumental task to solve the equation for the aligned-electron model, and we have presented full solutions on a numerical grid [13]. The double-ionization yield given by these solutions [14] showed the familiar knee structure for DI, suggesting that the one-dimensional model contains the essential physics for DI.

In examining the time development of double ionization [13], we could clearly see "jets" of DI occurring during each half laser cycle, but their physical origins were not obvious. Even the aligned-electron model is complicated enough that it is not clear from a numerical solution precisely which processes are occurring. It was for this reason that we introduced quantum-mechanical masking, in which a portion of the population is "masked" so that the time development of a different

portion can be studied separately. In particular, we masked the population that had both electrons close to the nucleus at a chosen time and traced the time development of the portion of the wavefunction that had one electron away from the nucleus at that chosen time [6]. The unmasked population clearly showed the detached electron returning to the core area—an indicator for recollision—and subsequent DI.

## 3. MASKING

In our earlier papers, we focused on results and did not include a detailed description of the masking procedure. Consequently, we include a more complete description here. We begin by evolving the system's full wavefunction from  $t = 0$  until some chosen time  $t = t_0$ , using the propagator  $U$ :

$$\Psi(t_0) = U(t_0, 0)\Psi(0).$$

We then separate  $\Psi(t_0)$  into two or more components. For a case in which we separate it into three parts, we can write

$$\Psi(t_0) = \Psi_1(t_0) + \Psi_2(t_0) + \Psi_3(t_0).$$

These parts are each evolved separately, using the same full propagator:

$$\Psi_n(t) = U(t, t_0)\Psi_n(t_0).$$

For numerical wavefunctions on a grid, these independent evolutions are performed on the full grid using the same propagator as for the full wavefunction. Because of the linearity of the time-dependent Schrödinger equation, the full wavefunction can be constructed at any chosen time  $t$  as the sum of the components:

$$\begin{aligned} \Psi(t) &= U(t, t_0)\Psi(t_0) \\ &= U(t, t_0)[\Psi_1(t_0) + \Psi_2(t_0) + \Psi_3(t_0)] \\ &= \Psi_1(t) + \Psi_2(t) + \Psi_3(t). \end{aligned}$$

The modulus squared of the wavefunction is the sum of the moduli squared of the masked wavefunctions, plus interference terms.

In our studies involving a spatial wavefunction on a grid, we have based the separation on regions of the  $(x_1, x_2)$  plane, but we emphasize that the separation of the wavefunction can be done for a variety of criteria, including energy and momentum. Basically, any decomposition of the state vector that is desired can be used. We use the term "masking" because it implies that there is something else present but hidden. The quantum state vector is a coherent superposition of complex amplitudes for all available processes, and the full wavefunction is always the coherent sum of the masked and unmasked portions.

Writing a wavefunction or state vector as a sum of component state vectors with different quantum histories is by no means a new idea in quantum mechanics. One very obvious example is writing the state vector for

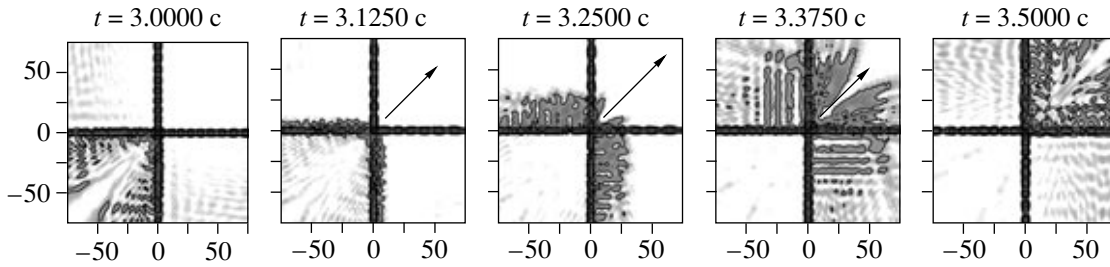


**Fig. 1.** Modulus squared of the full wavefunction vs. position coordinates  $x_1$  and  $x_2$  from  $t = 3$  to  $3.5$  c, and reproducing Fig. 1 of Ref. [6]. The plot is logarithmic, with shading beginning at  $4 \times 10^{-7}$  and contour lines starting at  $10^{-6}$  and each order of magnitude thereafter. The arrow indicates the strength and effective direction of the laser force on the electrons. The pulse is trapezoidal, with two-cycle turn-on and turn-off. The laser intensity is  $6.5 \times 10^{14}$  W/cm<sup>2</sup>, and the frequency is 0.0584 au.

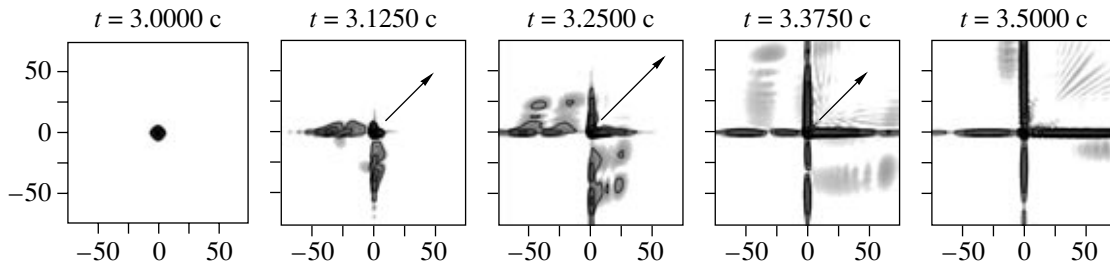


**Fig. 2.** Time development of a masked wavefunction from  $t = 3$  to  $3.5$  c. The mask keeps only the population at a radius  $(x_1^2 + x_2^2)^{1/2}$  of less than 6 au. We use a smooth cutting function of width 1 au. The double ionization is explainable in terms of recollisions that occur at about  $t = 3$  c.

a double-slit apparatus as the sum of state vectors for propagation through each slit. Of course, in this example, the interference effects provide some very important physics! The usefulness of the technique depends very much on the size of the interference terms. Strong-field DI behaves very classically and is a good context for using masking.

In Fig. 1 we see the time development of the modulus squared of the system's spatial wavefunction versus positions  $x_1$  and  $x_2$  from  $t = 3$ – $3.5$  laser cycles for a six-cycle laser pulse. This figure serves as our “baseline” double-ionization sequence and corresponds with Fig. 1 of [6]. The population near the origin has both electrons near the nucleus. The population away from the origin but near an axis has one electron highly excited or ionized. The population well away from both axes represents DI. Major features to note in the figure include the double-ionization jets, which emerge from near the origin each half cycle approximately when the laser field is maximal, and the pulses of population that emerge from along the axes into the second and fourth quadrants immediately before the jets. Also note the  $x_1 \leftrightarrow x_2$  exchange symmetry. The ground state has this property, and the Hamiltonian preserves the symmetry.

#### 4. SYMMETRY-PRESERVING MASKS

In [6], where we introduced masking, we divided the  $t = 3$  c wavefunction into three components. These components, and the subsequent time development of each, are shown in Figs. 2–4. One component had both electrons close to the origin (Fig. 2) and has not previously been shown. A second component (Fig. 3) had one electron separated from the core, positioned so that it could return to the core with the laser force during the next half cycle. The third component (Fig. 4) had one electron away from the core and positioned to return against the laser force, i.e., while slowing down. We found that the DI was dominated by the third component and its slowdown collisions. We inferred some of the dynamics of these slowdown collisions through studying classical ensembles [15]. We found that the most effective recollision events occur when there is a good phase match between the motions of the inner and returning electron, so that the returning electron can exert maximal force over maximal distance. We have also found that it is very rare for both electrons to have energy greater than zero immediately after recollision. The final emergence of one or both particles was over a suppressed potential-energy barrier. Thus, there was often a time lag between the recollision event and emergence.

The speedup collisions shown in Fig. 3 were the primary topic of a follow-up paper [16] that presented evi-

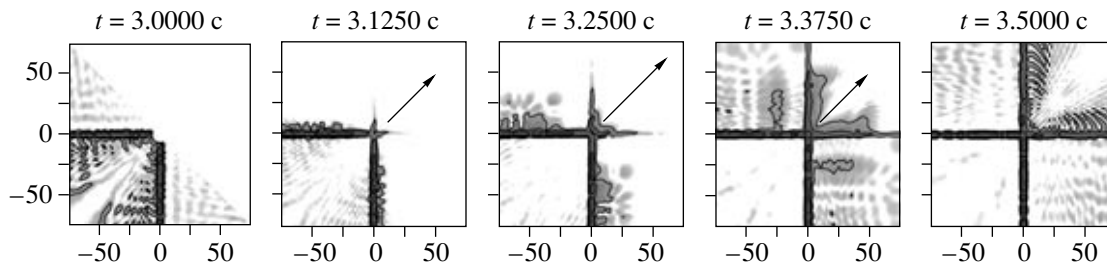


**Fig. 3.** Time development of a masked wavefunction from  $t = 3$  to  $3.5$  c. The mask keeps only population at radius  $(x_1^2 + x_2^2)^{1/2}$  greater than 6 au with  $x_1 + x_2 < 0$ . This population leads to speedup collisions and does not contribute significantly to the double ionization.

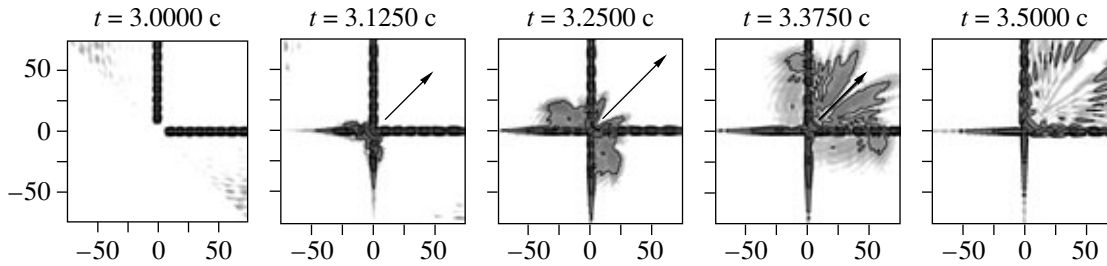


**Fig. 4.** Time development of a masked wavefunction similar to that of Fig. 3, but with  $x_1 + x_2 > 0$ . This population leads to slowdown collisions and dominates the double ionization.

dence that, for these collisions, the outer electron need never be ionized (i.e., have energy  $>0$ ) prior to the recollision.

The inner component of the wavefunction is shown in Fig. 2. After the mask is applied, some of the population moves against the laser force onto the positive axes. This motion is explainable in terms of the inertia of the population that has traveled out from the core but has returned so that both electrons are within 6 au of the nucleus at the instant the mask is applied. We emphasize that Fig. 2 shows that the recollisions occurring when the field is minimal do not lead to immediate DI jets in the direction of the recollision. Instead, the population remains near the axes—i.e., one electron remains near the core immediately after the collision. It escapes only as the field increases in strength. In our classical modeling, we saw that this second emergence is over a suppressed barrier [15].

To compare the populations associated with the various processes, we have calculated the  $t = 3.375$  c populations for which both electrons are between 10 au and 75 au on the positive side of the nucleus (so that the population lies in the first quadrant of the corresponding plot). The population associated with the slowdown collisions is  $3.95 \times 10^{-3}$ , that with the speedup collisions is  $0.57 \times 10^{-3}$ , and that with the inner wavefunction  $0.33 \times 10^{-3}$ . These total to  $4.85 \times 10^{-3}$ . The corresponding population for the full wavefunction is  $5.09 \times 10^{-3}$ . The discrepancy between 4.85 and 5.09 is attributable to the interference terms discussed below. The

differences among the populations are less dramatic if we include populations in the other quadrants. The total DI population (calculated as having both electrons between 10 and 75 au) at  $t = 3.375$  c associated with the slowdown collisions is  $5.35 \times 10^{-3}$ . The corresponding number for the masked wavefunction shown in Fig. 4 (which includes population emerging from along the negative axes as well as the speedup collisions) is  $3.47 \times 10^{-3}$ , and, with the inner wavefunction,  $1.27 \times 10^{-3}$ . These total to  $10.09 \times 10^{-3}$ . The corresponding population for the full wavefunction is  $10.27 \times 10^{-3}$ .

In the above discussion we applied masks at one specific time. We can also apply a temporal sequence of masks so as to track particular populations through time in a semiclassical fashion. For example, we can check our statement that the DI shown in Fig. 2 arises from recollision. In order to be recolliding at about  $t = 3$  c, the outer electron would need to be away from the core during the previous zero of the laser field. (An electron that is ejected between  $t = 2.5$  and  $3.0$  c would be expected to be pushed away from the nucleus and to not return until after the laser field switches direction.) We thus apply a sequence of masks: the first at  $t = 2.5$  c and keeping only the inner population (i.e., with both electrons within 6 au of the nucleus), and the second at  $t = 3.0$  c, similar to that of Fig. 2. The subsequent evolution is shown in Fig. 5. The DI that had been present in Fig. 2 is now destroyed. A complementary run (not shown), in which we keep the outer population at  $t = 2.5$  c and the inner population at  $t = 3$  c restores the DI. We conclude that the DI of Fig. 2 arose

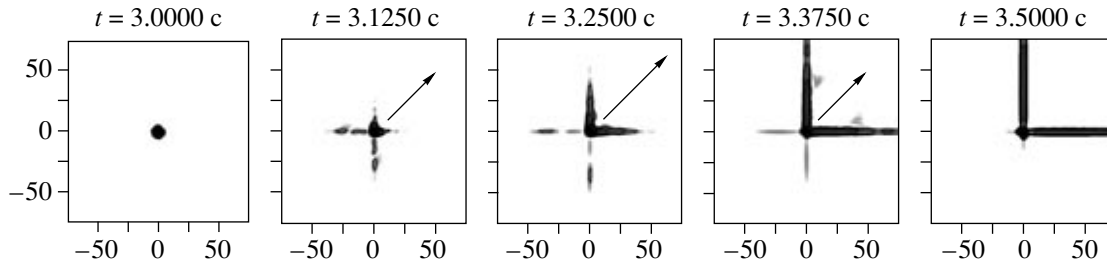


**Fig. 5.** Time development of the modulus squared of the wavefunction after applying a temporal sequence of masks. Both masks kept only the inner portion of the wavefunction  $[(x_1^2 + x_2^2)^{1/2} < 6 \text{ au}]$ . The first mask was applied at  $t = 2.5 \text{ c}$ , and the second, at  $t = 3.0 \text{ c}$ . Applying the earlier mask has caused the double ionization that was present in Fig. 2 to be hidden.

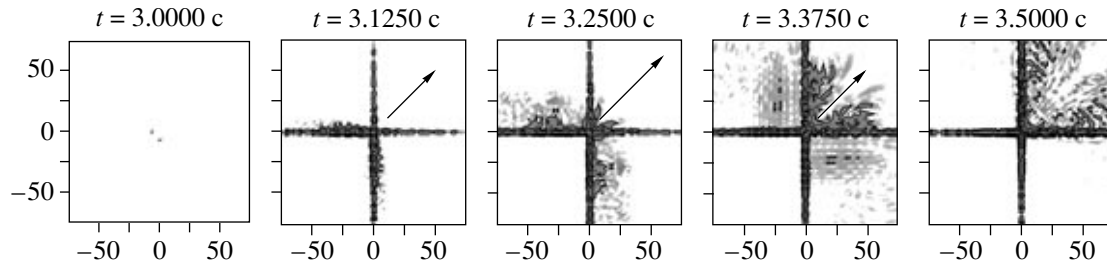


**Fig. 6.** Absolute value of the interference terms between masked wavefunctions of Figs. 2–4 on the same logarithmic scale. Although each of Figs. 2–4 represents a full solution of the time-dependent Schrödinger equation for the relevant “initial” conditions at  $t = 3 \text{ c}$ , the interference effects must be included to reconstruct Fig. 1, which shows the probability distribution of the entire system.

from recollision from a population that was away from the core at  $t = 2.5 \text{ c}$ .

We can also use a temporal sequence of masks to understand the DI evident in Fig. 4 as pulses of population emerging from along the negative axes into the second and fourth quadrants. This DI results from population that was away from the origin at  $t = 2.5 \text{ c}$  and that then returned to the core slightly before  $t = 3.0 \text{ c}$  and overshot. We infer that an energy-transferring recollision occurred shortly before the zero of the laser field. The inner electron apparently did not receive enough energy for immediate emergence, but it can emerge as the laser field grows stronger and the barrier becomes suppressed.

The full wavefunction can be calculated as the sum of the individual masked wavefunctions. The modulus squared of the sum can include cross terms or interference among the various components. The absolute values of interference terms among the wavefunctions of Figs. 2–4 are shown in Fig. 6. They are most important in areas where there is the most overlap among the masked wavefunctions, namely, along the axes and extending into the third quadrant. We have checked that Fig. 1 is regained by summing Figs. 2–4 and Fig. 6 (taking into account the proper signs for the interference terms). The existence of these interference terms serves as a good reminder that we are dealing with a quantum-mechanical system, not a classical ensemble of parti-

cles. Masking is not just a classical filter that selects out certain trajectories. Nonetheless, it is also true that all of the sequences in Figs. 2–4 represent full solutions of the time-dependent Schrödinger equation for the “initial” conditions imposed by the masks at  $t = 3 \text{ c}$ . The interference terms are necessary for reconstructing the full quantum-mechanical wavefunction for our system, which started in the ground state at  $t = 0$ , but they do nothing to undermine the basic conclusions that slow-down collisions are responsible for the majority of double-ionization jets in our system for these laser parameters.

## 5. SYMMETRY-BREAKING MASKS

In all of the above masks, we preserved the electron-exchange symmetry of the full wavefunction. Now, we apply some masks that break that symmetry. In Fig. 7 we begin as if to reproduce Fig. 4 for the slowdown collisions, but then we apply an additional mask that shows only the portion of the  $t = 3.0 \text{ c}$  wavefunction for which  $x_1 > x_2$ . We now have an outer ( $x_1$ ) and an inner ( $x_2$ ) electron. Thus, we provide a very classical description of the subsequent events. By  $t = 3.125 \text{ c}$ , some population has returned to the origin and has overshot. The population remains close to the axes after the recollision, indicating that only one electron is away from the nucleus. The overshoot along the  $x_1$  axis indicates that the *returning* electron has overshot. The part of the pop-

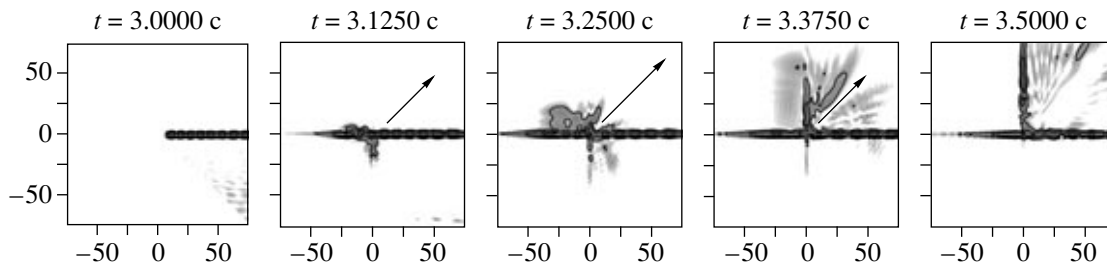


**Fig. 7.** Modulus squared of the spatial wavefunction after applying a mask that keeps only the population for which  $x_1 + x_2 > 0$  and  $x_1 > x_2$  at  $t = 3$  c. When the population returns to the origin, we have both overshoot of the returning electron and electron interchange. The more prominent DI jet evident at  $t = 3.375$  c has  $x_1 < x_2$  and, thus, consists primarily of population for which the outer ( $x_1$ ) electron follows the inner ( $x_2$ ) electron out. The sequence also shows electron interchange, in which the  $x_1$  electron becomes bound and the  $x_2$  electron is ionized.

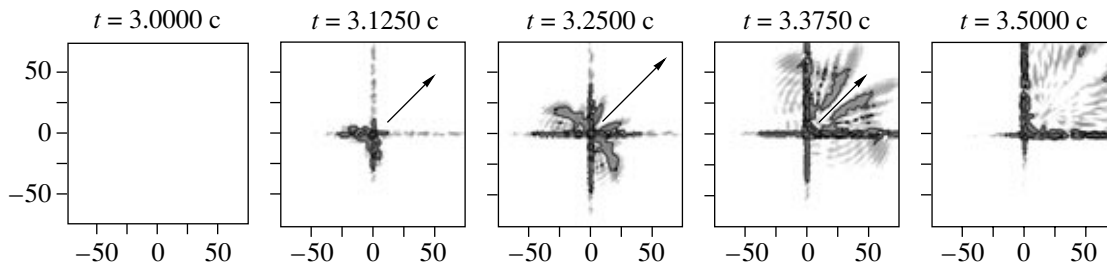


**Fig. 8.** Absolute value of interference effects between the wavefunction of Fig. 7 and its exchange complement.

ulation that moves onto the negative  $x_2$  axis has the other electron pushed out, indicating that an exchange has occurred.

By  $t = 3.25$  c, double ionization is occurring along the negative  $x_1$  axis. The inner ( $x_2$ ) electron is leaving the core area in the direction of the laser force, with the outer electron still having overshoot the nucleus. The  $t = 3.375$  c plot shows a sizable portion of a DI jet emerging from the vicinity of the origin. Interestingly, it predominantly has  $x_1 < x_2$ , indicating that the  $x_2$  electron (which had been the inner electron) is leading the other electron out. To summarize, the outer electron comes back to the core against the laser force, recollides and overshoots, and then comes back to the core again. In the majority of cases, this electron then follows the inner electron out in the direction of the laser force. These results are precisely what we saw for the dynamics of typical slowdown collisions in our classical studies [15]. It is interesting to notice that a considerable population lies on the positive  $x_2$  axis at  $t = 3.5$  c. For this population, the recollision did not lead to double ionization but rather to an electron interchange in which the outer ( $x_1$ ) electron came back to the core and was recaptured, while the other ( $x_2$ ) electron escaped in the direction of the laser force.

As the final step of setting up the sequence in Fig. 7, we applied a mask that showed only the population for which  $x_1 > x_2$ . A complementary masked wavefunction would be obtained if we applied a final mask for which

$x_1 < x_2$ . A plot of the subsequent time development would generate a sequence identical to Fig. 7 except for an interchanging of  $x_1$  and  $x_2$ . The sum of the two wavefunctions reproduces the wavefunction of Fig. 4, which shows the slowdown collisions. However, because the two wavefunctions share some region of support, interference effects between them must not be ignored. The interference effects are shown in Fig. 8. These interference effects are significant enough that we would need to be cautious about making quantitative predications from Fig. 7, but the conclusions drawn above appear safe.

Next, we consider a symmetry-breaking mask for the speedup collisions. If we keep only the population with  $x_1 < x_2$ , we obtain the result shown in Fig. 9. Recollision occurs, but it is perhaps striking how little DI occurs after the recollision. There is a small “bulge” into the first quadrant at  $t = 3.375$  c, but, for the most part, the population simply stays on the  $x_1$  axis. The absence of population along the  $x_2$  axis suggests that, predominantly, the returning electron overshoots the nucleus. Nonetheless, a numerical check reveals a non-zero population along the  $x_2$  axis; there simply is not enough to be seen in the graph.

If we sum the wavefunction of Fig. 9 and its exchange complement (for which  $x_1 > x_2$  at the time of the mask) and, then, calculate the modulus squared, we obtain the wavefunction of Fig. 3, which showed speedup collisions. Figure 10 shows the absolute value

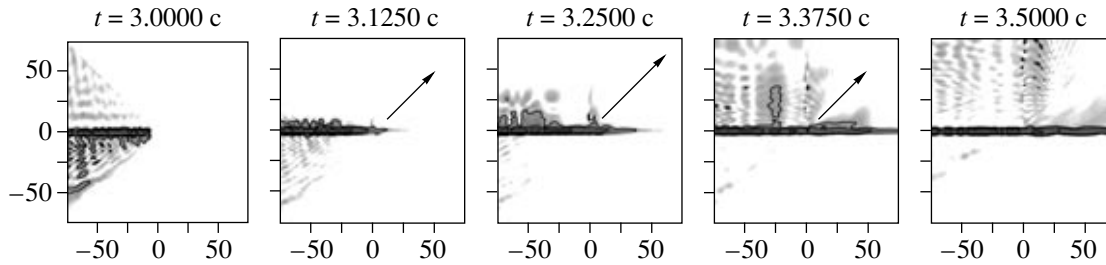


**Fig. 9.** Similar to Fig. 7, but the mask shows only the population for which  $x_1 + x_2 < 0$  and  $x_1 < x_2$  at  $t = 3$  c. Most of the population that returns to the core in the speedup collisions simply overshoots, with little DI or electron interchange occurring. Some interchange does occur, but it is below the scale of the graph.

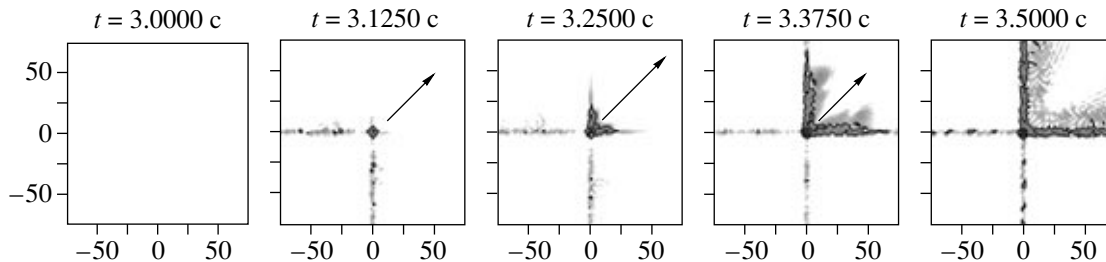


**Fig. 10.** Absolute value of the interference terms between the wavefunction of Fig. 9 and its exchange ( $x_1 \longleftrightarrow x_2$ ) complement. The interference terms are important for reproducing the speedup jets visible in Fig. 4.

of the interference terms. And now we find something possibly surprising—the interference terms are important along both positive axes. One wavefunction in the sum is much greater than the other, but the other is non-zero, and their product is large enough to be important on the graph. We also note that the “speedup jets” that can be seen in Fig. 3 would not be expected just from Fig. 9, where there was merely a small bulge into the first quadrant, and neither are they clearly evident in the interference terms. We infer that electron interchange—in which the returning electron transfers a large fraction of its energy to the other electron—plays an important role in the formation of these “speedup jets” and also that the quantum interference between the two should not be ignored.

## 6. CONCLUSIONS

We have presented the quantum-mechanical technique of masking and shown its usefulness in studying strong-field double ionization. Through masking we are able to separate various populations and study their individual time development. We have reviewed earlier examinations of speedup and slowdown collisions, and we have presented the other components of the full probability distribution, including terms that represent interference among the masked components. While the interference terms are certainly important for reconstructing the full probability distribution, they do not affect the fundamental physics of the speedup or slowdown collisions. For the laser intensity and frequency

considered here, the excess double ionization is fully explainable in terms of recollision. The slowdown collisions dominate in our model for the laser parameters employed, but collisions at other laser phases also contribute.

We have extended the masking technique to allow for masks that break the electron-exchange symmetry, thereby allowing a very classical tracking of each electron. We have found that the slowdown collisions exhibit a sequence of events very similar to what is found in classical ensembles, with the returning electron typically recolliding and overshooting the core before being pushed back toward the core by the laser and following the other electron out in the direction of the laser force. We also have noted that electron interchange also occurs, in which the electrons switch roles.

This paper is dedicated to my collaborator, Professor J.H. Eberly. In preparing this manuscript I have performed new computer runs and assembled the results. I have rounded out what we previously coauthored with our students by presenting details of the masking procedure and showing interference terms, and I have extended the analysis to allow for symmetry-breaking masks. I have independently written this paper so that I can properly include it in this special issue, but I want to be very clear that this paper could never have been written without the benefits of the Calvin–Rochester collaboration. This paper should be seen as a presentation of results that arise from the collaboration and that is dedicated to Joe; it should not be seen as a stand-alone investigation.

## ACKNOWLEDGMENTS

This work has been supported by the National Science Foundation through Grant PHY-0355035 to Calvin College. I also wish to reiterate my acknowledgement of the invaluable contributions of K. Hoekema, R. Panfili, and J.H. Eberly to this work.

## REFERENCES

1. S. L. Haan, R. Grobe, and J. H. Eberly, *Phys. Rev. A* **50**, 378 (1994).
2. J. Javaneinen, J. H. Eberly, and Qichang Su, *Phys. Rev. A* **38**, 3430 (1988); Q. Su and J. H. Eberly, *Phys. Rev. A* **44**, 5997 (1991).
3. J. Javaneinen (in press); R. Grobe and Q. Su (in press).
4. R. Grobe and J. H. Eberly, *Phys. Rev. A* **48**, 4664 (1993).
5. M. S. Pindzola, D. C. Griffin, and C. Bottcher, *Phys. Rev. Lett.* **66**, 2305 (1991); J. B. Watson, A. Sanpera, D. G. Lappas, *et al.*, *Phys. Rev. Lett.* **78**, 1884 (1997); D. Bauer, *Phys. Rev. A* **56**, 3028 (1997); A. M. Popov, O. V. Tikhonova, and E. A. Volkova, *Opt. Express* **8**, 441 (2001); M. Lein, E. K. U. Gross, and V. Engel, *Phys. Rev. Lett.* **85**, 4707 (2000); Nils Erik Dahlen and Robert van Leeuwen, *Phys. Rev. A* **64**, 023 405 (2001).
6. S. L. Haan, P. S. Wheeler, R. Panfili, and J. H. Eberly, *Phys. Rev. A* **66**, 061402(R) (2002).
7. A. Becker and F. H. M. Faisal, *J. Phys. B* **29**, L197 (1996); F. H. M. Faisal and A. Becker, *Laser Phys.* **7**, 684 (1997).
8. J. Parker, K. T. Taylor, C. W. Clark, and S. Blodgett-Ford, *J. Phys. B* **29**, L33 (1996); J. Parker, E. S. Smyth, and K. T. Taylor, *J. Phys. B* **31**, L571 (1998).
9. R. Dörner, Th. Weber, M. Weckenbrock, *et al.*, *Adv. At. Mol. Opt. Phys.* **48**, 1 (2002).
10. D. N. Fittinghof, P. R. Bolton, B. Chang, and K. C. Kulander, *Phys. Rev. Lett.* **69**, 2642 (1992); B. Walker, B. Sheehy, L. G. DiMauro, *et al.*, *Phys. Rev. Lett.* **73**, 1227 (1994).
11. M. V. Ammosov, N. B. Delone, and V. P. Krainov, *Sov. Phys. JETP* **64**, 1191 (1986).
12. K. J. Schafer, B. Yang, L. F. DiMauro, and K. C. Kulander, *Phys. Rev. Lett.* **70**, 1599 (1993); P. B. Corkum, *Phys. Rev. Lett.* **71**, 1994 (1993).
13. S. L. Haan, N. Hoekema, S. Poniatowski, *et al.*, *Opt. Express* **7**, 29 (2000).
14. W.-C. Liu, J. H. Eberly, S. L. Haan, and R. Grobe, *Phys. Rev. Lett.* **83**, 520 (1999).
15. R. Panfili, S. L. Haan, and J. H. Eberly, *Phys. Rev. Lett.* **89**, 113001 (2002).
16. S. L. Haan, J. C. Cully, and K. Hoekema, *Opt. Express* **12**, 4758 (2004).